RESEARCH PAPER

Flexural dynamic response of monopile foundations under linear wave loads

by Theofanis Giotis* [1], Dimitrios Pavlou [2]

[1,2] *University of Stavanger, Stavanger, Norway*

ARTICLE INFO

Received: *16 December 2019*
Accepted: *06 February 2020*

ABSTRACT

An analytical solution for the dynamic response of submerged slender circular cylindrical structures subjected to linear wave loads is presented. A double Laplace transform with respect to temporal and spatial variables is applied both to motion equation and boundary conditions. The dynamic deflection of the beam is obtained by inversion of the Laplace transform. The latter with respect to spatial variable is obtained analytically, while the one concerning the temporal variable is numerically calculated using Durbin numerical scheme. Results in the case of a representative example for a monopile foundation subjected to Airy waves are presented and discussed, and the analytical result is compared against numerical dynamic and static solutions.

Key words: Laplace transform, Morison Equation, dynamic response, monopile.

INTRODUCTION

The analysis of dynamic response of circular cylindrical structures under wave loads has attracted attention by many investigators. The focus is mainly on the determination of dynamic deflection obtained through numerical methods, and experimental studies in wave tank, e.g., [1]. In the present work an analytical solution for the dynamic response of slender cylindrical structures under Airy waves is presented, which is obtained by using Laplace transform techniques. The proposed solution has the advantage that the solution of the PDE is analytic and could be easily extended to include the additional effect of current.

The waves encountered in the installation area are characterized by a small steepness ratio H/λ and as a result they can be considered as linear. The monopile foundation is assumed fixed on the seabed. This assumption is valid for rocky or stiff seabed. The geometric characteristics of the pile remain constant throughout its length and the outer diameter $\left(D_{out}\right)$ of the foundation is small with respect to the wavelength (λ) of the installation area. The small ratio D/λ allows the assumption that the flow disturbance is not significant due to the presence of the structure and as a result, the monopile can be considered as a slender structure. The origin (O) of the system is located on the center of the foundation base (Fig. 1).

Analytical solution of the problem

Boundary conditions

The fixed end which is located on the seabed $z = 0$. Thus, slope and deflection are zero at $z = 0$.

$$w(0,t) = \left.\frac{\partial w(z,t)}{\partial z}\right|_{z=0} = 0 \tag{1}$$

The upper end at $z = L$ is free and as a result, both bending moment and shear force are zero at $z = L$.

$$\mathrm{E}\cdot\mathrm{I}(z)\cdot\left.\frac{\partial^2 w(z,t)}{\partial z^2}\right|_{z=L} = 0 \tag{2}$$

$$\frac{\partial}{\partial z}\left[\mathrm{E}\cdot\mathrm{I}(z)\cdot\frac{\partial^2 w(z,t)}{\partial z^2}\right]_{z=L} = 0 \tag{3}$$

*Corresponding author: Theofanis Giotis, e-mail: fanisgiotis@gmail.com.

http://doi.org/10.28999/2514-541X-2020-4-1-44-50

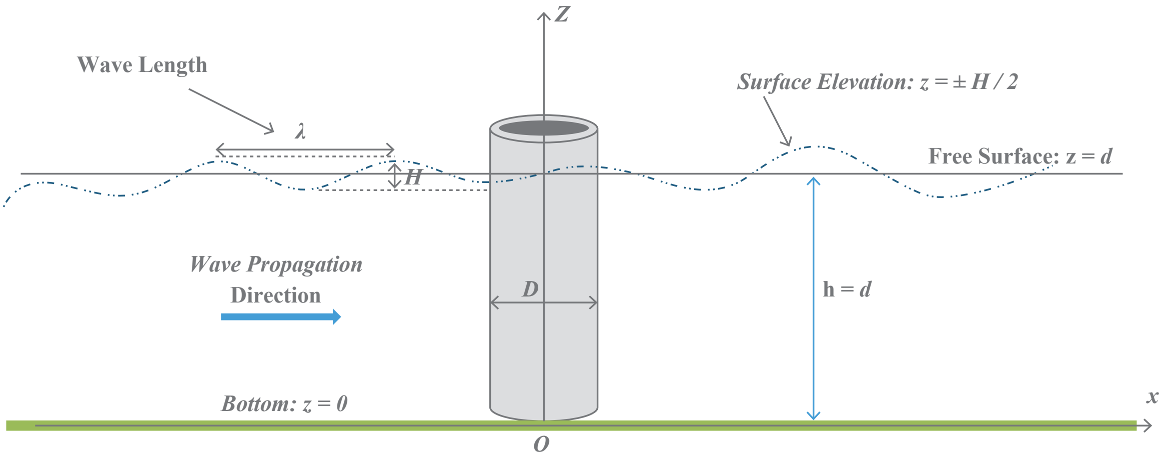

Figure 1. *The origin system of the monopile.*

Equation of motion

The dynamic displacement field is expressed by means of Euler-Bernoulli beam model [2]:

$$\mathrm{E}\cdot\mathrm{I}\cdot\frac{\partial^4 w(z,t)}{\partial z^4}+\mathrm{P}\cdot\mathrm{A}_C\cdot\frac{\partial^2 w(z,t)}{\partial t^2}+C\cdot\frac{\partial w(z,t)}{\partial t}=q(z,t) \tag{4}$$

The righthand side part of equation (4) is the hydrodynamic load calculated by using potential wave theory [3,4] and Morison Equation [5]. The circular cylinder is considered as a moving structure in waves. Thus, the relative formulation of Morison Equation is used. However, the structure represents a monopile offshore wind turbine, which has to be rigid enough for the safety of the rotor. The rigidity of the structure ensures that the maximum deflection amplitude is much smaller than the structure diameter (D_{out}), and as a result, the velocity of the structure could be neglected. The final form of the hydrodynamic load is given by Equation (5).

$$q(z,t)=-\rho\cdot C_{\mathrm{A}}\cdot\mathrm{A}\cdot\frac{\partial^2 w(z,t)}{\partial t^2}+\rho\cdot C_{\mathrm{M}}\cdot \mathrm{A}\cdot\frac{Du(t)}{Dt}+\frac{1}{2}\cdot\rho\cdot C_D\cdot D_{out}\cdot u(t)\cdot\left|u(t)\right| \tag{5}$$

The drag term of equation (5) is linearized and the final form of equation of motion is:

$$\mathrm{E}\cdot\mathrm{I}\cdot\frac{\partial^4 w(z,t)}{\partial z^4}+\left[\mathrm{P}\cdot\mathrm{A}_C+\rho\cdot C_{\mathrm{A}}\cdot\mathrm{A}\right]\cdot\frac{\partial^2 w(z,t)}{\partial t^2}+C\cdot\frac{\partial w(z,t)}{\partial t}=$$
$$-C_{\mathrm{M}}\cdot\rho\cdot\frac{\pi\cdot D_{out}^2}{4}\cdot\omega^2\cdot\frac{\mathrm{H}}{2}\cdot\frac{\cosh(k\cdot z)}{\sinh(k\cdot d)}\cdot\sin(\omega\cdot t)+\frac{1}{2}\cdot\rho\cdot C_D\cdot D\cdot\left[\frac{\mathrm{H}}{2}\cdot\omega\cdot\frac{\cosh(k\cdot z)}{\sinh(k\cdot d)}\right]^2\cdot\cos(\omega\cdot t) \tag{6}$$

General solution of the motion equation

For the solution of the boundary value problem, Laplace transform will be applied to the spatial and temporal variables. The definition of these transforms and their inverse forms used on the solution is given in the Appendix. Application of the Laplace transform with respect to time and introduction of $w^n(z,0)=0$ for $n=1,2,3,4$ yield:

$$\mathrm{E}\cdot\mathrm{I}\cdot\frac{\partial^4 \overline{w}(z,s)}{\partial z^4}+\overline{w}(z,s)\cdot\left[\left(\mathrm{P}\cdot\mathrm{A}_C+\rho\cdot C_{\mathrm{A}}\cdot\mathrm{A}\right)\cdot s^2+C\cdot s\right]=$$
$$-C_{\mathrm{M}}\cdot\rho\cdot\frac{\pi\cdot D_{out}^2}{4}\cdot\omega^3\cdot\frac{\mathrm{H}}{2}\cdot\frac{\cosh(k\cdot z)}{\sinh(k\cdot d)}\cdot\left(\frac{1}{s^2+\omega^2}\right)+\frac{1}{2}\cdot\rho\cdot C_D\cdot D\cdot\left[\frac{\mathrm{H}}{2}\cdot\omega\cdot\frac{\cosh(k\cdot z)}{\sinh(k\cdot d)}\right]^2\cdot\left(\frac{s}{s^2+\omega^2}\right) \tag{7}$$

Where:

$$\overline{w}(z,s)=\mathcal{L}\left\{w(z,t);t\rightarrow s\right\}=\int_0^\infty e^{-s\cdot t}\cdot w(z,t)\,dt \tag{8}$$

Application of the Laplace transform with respect to z and introduction of zero initial conditions into equation (7) yield:

Magnitude	Name	Value
Height (m)	h	30
Outer Diameter (m)	D_{out}	6
Shell Thickness (m)	thik	0.05
Modulus of Elasticity (GPa)	E	210
Poisson’s Ratio	v	0.30
Density of Material (kg/m³)	P	7820
Damping Coefficient	C	4398
Added Mass Coefficient	C_A	1
Drag Coefficient	C_D	0.65

Table 2. *Structural characteristics of the pile.*

Magnitude	Name	Value
Wave Height (m)	H	3.5
Wave Period (sec)	T	6
Water Depth (m)	d	30
Wavenumber	k	0.1121
Wave Frequency (rad/sec)	w	1.0472
Density of Water (kg/m³)	ρ	1024.7

Table 3. *Wave characteristics of the installation area.*

$$\mathrm{E}\cdot\mathrm{I}\cdot\left[-\overline{w}'''(0,s)-q\cdot\overline{w}''(0,s)-q^2\cdot\overline{w}'(0,s)-q^3\cdot\overline{w}(0,s)+q^4\cdot\overline{w}^*(q,s)\right]+$$
$$\left[(\mathrm{P}\cdot\mathrm{A}+\rho\cdot C_{\mathrm{A}}\cdot\mathrm{A})\cdot s^2+C\cdot s\right]\cdot\overline{w}^*(q,s)=$$
$$-C_{\mathrm{M}}\cdot\rho\cdot\frac{\pi\cdot D_{out}^2}{4}\cdot\omega^3\cdot\frac{\mathrm{H}}{2}\cdot\frac{1}{\sinh(k\cdot d)}\cdot\left(\frac{1}{s^2+\omega^2}\right)\cdot\left(\frac{q}{q^2-k^2}\right)+$$
$$\frac{1}{8}\cdot C_D\cdot\rho\cdot D_{out}\cdot\mathrm{H}^2\cdot\omega^2\cdot\frac{1}{\sinh^2(k\cdot d)}\cdot\left(\frac{s}{s^2+\omega^2}\right)\cdot\frac{q^2-2\cdot k^2}{q\cdot(q^2-4\cdot k^2)} \tag{9}$$

Where:

$$\overline{w}^*(q,s)=\mathcal{L}\left\{\overline{w}(z,s);z\to q\right\}=\int_0^\infty e^{-q\cdot z}\cdot\overline{w}(z,s)\cdot dz \tag{10}$$

For the simplification of equation (9), the Laplace transform is applied into the boundary conditions equation (2). Thus, the conditions at $z=0$ takes the following form:

$$\overline{w}(0,s)=\mathcal{L}\left\{w(0,t);t\to s\right\}=0 \tag{11}$$

$$\overline{w}'(0,s)=\mathcal{L}\left\{w'(0,t);t\to s\right\}=0 \tag{12}$$

Introducing equations (11), (12) into equation (9) yields:

$$\overline{w}^*(q,s)\cdot\left[\mathrm{E}\cdot\mathrm{I}\cdot q^4+(\mathrm{P}\cdot\mathrm{A}_C+\rho\cdot C_{\mathrm{A}}\cdot\mathrm{A})\cdot s^2+C\cdot s\right]$$
$$=\mathrm{E}\cdot\mathrm{I}\cdot q\cdot\overline{w}''(0,s)+\mathrm{E}\cdot\mathrm{I}\cdot\overline{w}'''(0,s)-$$
$$C_{\mathrm{M}}\cdot\rho\cdot\frac{\pi\cdot D_{out}^2}{4}\cdot\omega^3\cdot\frac{\mathrm{H}}{2}\cdot\frac{1}{\sinh(k\cdot d)}\cdot\left(\frac{1}{s^2+\omega^2}\right)\cdot\left(\frac{q}{q^2-k^2}\right)+$$
$$\frac{1}{8}\cdot C_D\cdot\rho\cdot D_{out}\cdot\mathrm{H}^2\cdot\omega^2\cdot\frac{1}{\sinh^2(k\cdot d)}\cdot\left(\frac{s}{s^2+\omega^2}\right)\cdot\frac{q^2-2\cdot k^2}{q\cdot(q^2-4\cdot k^2)} \tag{13}$$

Solving equation (13) with respect to $\overline{w}^*(q,s)$, yields:

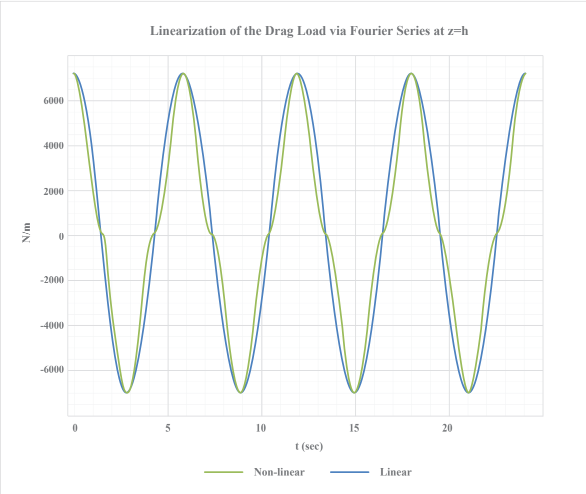

Figure 2. *Linear and non-linear drag load at z=h.*

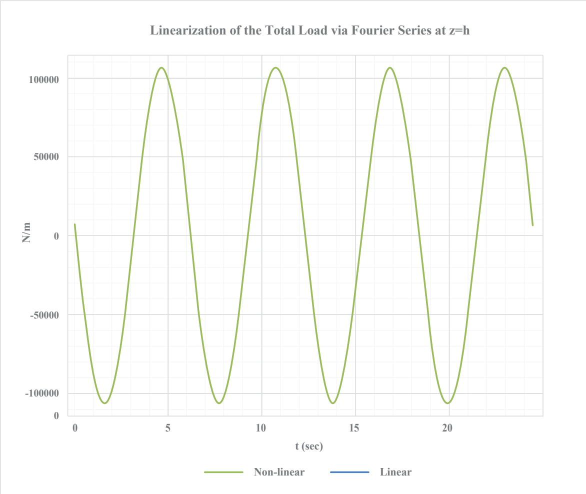

Figure 3. *Linear and non-linear total load at z=h.*

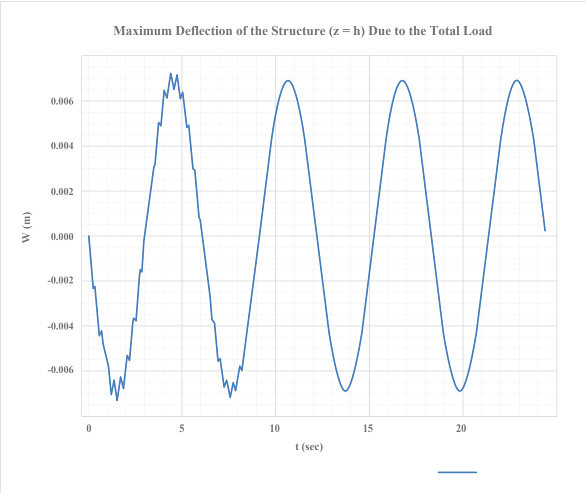

Figure 4. *Deflection of the structure at z=h.*

$$\bar{w}^*(q,s)=\bar{\mathrm{M}}_1^*(q,s)\cdot\bar{w}''(0,s)+\bar{\mathrm{M}}_2^*(q,s)\cdot\bar{w}'''(0,s)+\bar{\mathrm{M}}_3^*(q,s)+\bar{\mathrm{M}}_4^*(q,s) \tag{14}$$

where $\bar{\mathrm{M}}_1^*(q,s), \bar{\mathrm{M}}_2^*(q,s), \bar{\mathrm{M}}_3^*(q,s), \bar{\mathrm{M}}_4^*(q,s)$ are given in [9].

Application of the inverse Laplace transform with respect to q into equation (14) yields:

$$\bar{w}(z,s)=\bar{\mathrm{M}}_1(z,s)\cdot\bar{w}''(0,s)+\bar{\mathrm{M}}_2(z,s)\cdot\bar{w}'''(0,s)+\bar{\mathrm{M}}_3(z,s)+\bar{\mathrm{M}}_4(z,s) \tag{15}$$

Where

$$\bar{w}(z,s)=\mathcal{L}^{-1}\left\{\bar{w}^*(q,s);q\to z\right\} \tag{16}$$

$$\bar{\mathrm{M}}_i(z,s)=\mathcal{L}^{-1}\left\{\bar{\mathrm{M}}_i^*(q,s);q\to z\right\},\quad i=1,2,3,4 \tag{17}$$

Equation (15) contains two unknown variables $\bar{w}''(0,s)$ and $\bar{w}'''(0,s)$. The first expresses the bending moment at the position $z = 0$ and the second is equal with the shear force at the base of the foundation ($z = 0$). The determination of those variables is achieved by the introduction of the boundary conditions of the beam at the position $z = L$. Application of the Laplace transform with respect to time into equations (2) and (3) yields:

$$\bar{w}''(L,s)=\mathcal{L}\left\{w''(L,t);t\to s\right\}=0 \tag{18}$$

$$\bar{w}'''(L,s)=\mathcal{L}\left\{w'''(L,t);t\to s\right\}=0 \tag{19}$$

Application of the inverse Laplace transform with respect to s into equation (15) finally yields:

$$w(z,t)=\mathcal{L}^{-1}\left\{\bar{\mathrm{M}}_1(z,s)\cdot\bar{w}''(0,s)+\bar{\mathrm{M}}_2(z,s)\cdot\bar{w}'''(0,s)+\bar{\mathrm{M}}_3(z,s)+\bar{\mathrm{M}}_4(z,s);s\to t\right\} \tag{20}$$

Where:

$\bar{w}''(0,s)$ and $\bar{w}'''(0,s)$ are given in [9], and

$$w(z,t)=\mathcal{L}^{-1}\left\{\bar{w}(z,s);s\to t\right\} \tag{21}$$

Linearization of the hydrodynamic load

It is important to mention that the equation which describes the horizontal Drag load on strip is a non-linear equation. The analytical calculation of the pylon response under the horizontal wave loads requires the formulation of the load equation as the addition of linear harmonic terms. It can be achieved by developing the Drag load into a Fourier series. The process of converting the Drag load into a sum of linear harmonic terms is described in detail as follows.

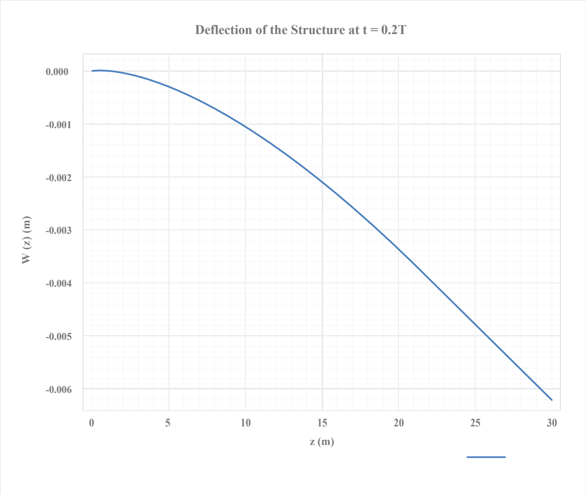

Figure 5. *Deflection of the structure at t=0.2T.*

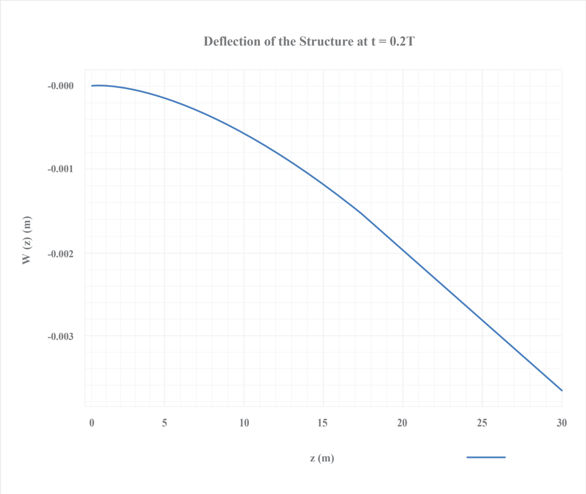

Figure 6. *Deflection of the structure at t=0.4T.*

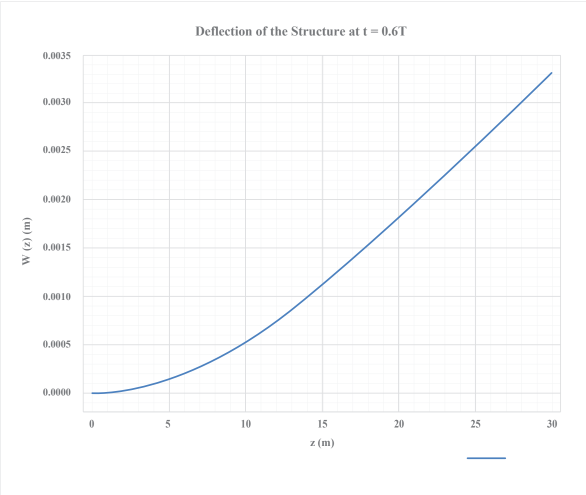

Figure 7. *Deflection of the structure at t=0.6T.*

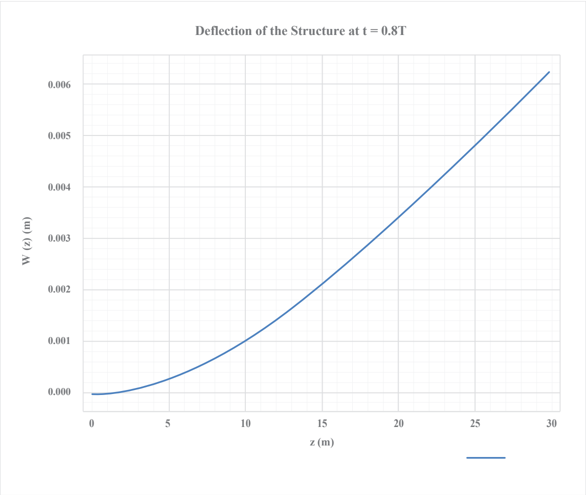

Figure 8. *Deflection of the structure at t=0.8T.*

Non-linear term could be written as an independent function named N.

$$\mathrm{N} = C_2 \cdot \left|\cos\left(k \cdot x_c - \omega \cdot t\right)\right| \cdot \cos\left(k \cdot x_c - \omega \cdot t\right) \qquad (22)$$

Where:

$$C_2 = \frac{1}{2} \cdot \rho \cdot C_D \cdot D_{out} \cdot \left[\frac{\mathrm{H}}{2} \cdot \omega \cdot \frac{\cosh\left[k \cdot \left(z + d\right)\right]}{\sinh\left(k \cdot d\right)}\right]^2$$

By setting $0 = k \cdot x_c - \omega \cdot t$, equation (22) takes the following form:

$$\mathrm{N}\left(\theta\right) = C_2 \cdot \left|\cos\left(\theta\right)\right| \cdot \cos\left(\theta\right) \Rightarrow \mathrm{N}\left(\theta\right)$$

$$= \begin{cases} C_2 \cdot \cos^2\left(\theta\right), -\dfrac{\pi}{2} \le \theta \le \dfrac{\pi}{2} \\ -C_2 \cdot \cos^2\left(\theta\right), \dfrac{\pi}{2} \le \theta \le \dfrac{3\pi}{2} \end{cases} . \qquad (23)$$

Let as now consider the representation of $\mathrm{N}\left(\theta\right)$ in a Fourier series as follows:

$$\frac{\mathrm{N}\left(\theta\right)}{C_2} = \frac{1}{2} \cdot a_0 + \sum_{j=1}^{\infty} a_j \cdot \cos\left(j \cdot \theta\right) + \sum_{j=1}^{\infty} b_j \cdot \sin\left(j \cdot \theta\right)$$

Where:

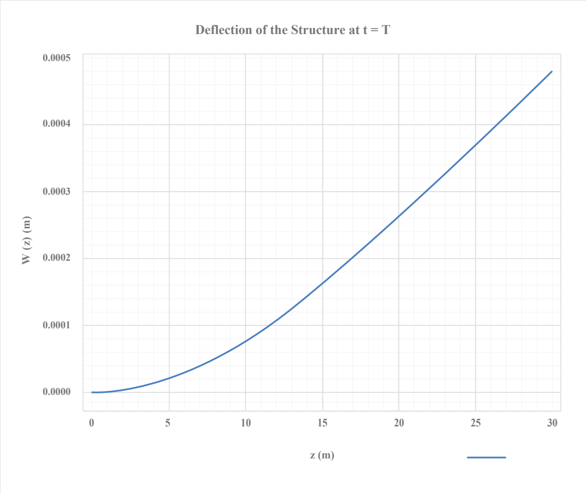

__Figure 10.__ Comparison between maximum static and the dynamic deflection.

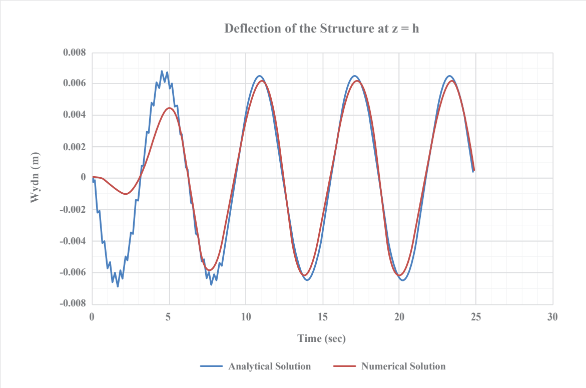

__Figure 11.__ Comparison between numerical and analytical solution.

$$a_j = \frac{2}{\pi} \cdot \int_0^T \mathrm{N}(\theta) \cdot \cos(j \cdot \theta) \cdot d\theta,$$

and

$$b_j = \frac{2}{\pi} \cdot \int_0^T \mathrm{N}(\theta) \cdot \sin(j \cdot \theta) \cdot d\theta.$$

In the case when $a_0 = 0$ and $|a_j| << |a_1|$, and $|b_j| << |b_1|$, for $j > 1$, as happens to be the ones considered here, the function $\mathrm{N}(\theta)$ is approximated by using only the first term in the series as follows:

$$\frac{\mathrm{N}(\theta)}{C_2} \approx a_1 \cdot \cos(\theta), \text{ with } a_1 = \max\left|\frac{\mathrm{N}(\theta)}{C_2}\right| \tag{24}$$

Using the above approximation in equation (5) we finally obtain:

$$\frac{dF_{\mathrm{N}_D}(t)}{dz} \approx \frac{1}{2} \cdot \rho \cdot C_D \cdot D_{out} \cdot \left[\frac{\mathrm{H}}{2} \cdot \omega \cdot \frac{\cosh\left[k \cdot (z+d)\right]}{\sinh(k \cdot d)}\right]^2 \cdot \cos(k \cdot x_c - \omega \cdot t) \tag{25}$$

Numerical example of the analytical solution

A vertical circular cylindrical structure, fixed in the seabed is considered, as described by Table 2.

The wave characteristics of the installation area of the structure are given in Table 3.

The comparison of the non-linear drag load at the top of the structure $(z = h)$ and its linearized approximation by means of equation (25) is presented in Fig. 2.

Applying the Morison Equation for both linear and non-linear drag load, the total hydrodynamic load on the top of the structure $(z = h)$ is presented in Fig. 3.

Applying equation (20), the deflection of the structure at $z = h$, during four periods, is given in Fig. 4.

The response of the structure at $z = h$ follows the form of the total hydrodynamic load. Deflection is equal with zero at $t = 0$ due to the zero initial conditions used during the analytical solution. Thus, the maximum dynamic deflection of the beam is equal to $w(L)_{Dynamic} = 0.0064$ m. The calculated deflection of the pillar due to the hydrodynamic load is presented in Fig 5–9.

Evaluation of the analytical solution

Comparison between analytical dynamic and static solution

To verify the reliability of the results, the dynamic deflection of the structure due to the hydrodynamic load, is compared with the maximum static deflection. The solution of the static problem is achieved by using the finite element method (FEM). The maximum static deflection is $w(L)_{Static}$ = 0.0064 m, and compared with the maximum dynamic deflection, they are equal. The dynamic deflection of the beam with respect to the maximum static deflection due to the hydrodynamic load, is presented in Fig. 10.

Comparison between analytical and numerical solution

For the validation of the present analytical model, the problem is also solved numerically by a Finite Differential Method, and the comparison between the numerical and analytical solution is presented in Fig. 11.

The numerical solution with FDM, verifies that the analytical solution is characterized by high accuracy.

Conclusions

In this work the calculation of wave loads on monopile foundations is presented, as obtained by application of Morison Equation, in conjunction with potential flow theory. Results of representative examples for a monopile foundation subjected to short waves are presented and discussed. Subsequently, the elastic response of the vertical pillar in waves is studied and an analytical solution concerning the dynamic response is also derived based on linearization. For the validation of the present method, a numerical solution for the dynamic response of the monopile foundation subjected to general wave loads is derived, based on finite difference method (FDM). The numerical and the analytical solution give approximately the same result, verifying the accuracy of the analytical solution for waves of relatively small amplitude. Moreover, the calculation of the maximum static deflection of the structure subjected to the maximum wave loads is obtained by the finite element method (FEM) and is found compatible with the amplitude of analytical dynamic deflection.

Future work includes the introduction of current effects and wind loads into the analytical and numerical model which is important for a more efficient and realistic estimation of the dynamic response of such structures. Also, the developed analytical solution is realistic in the case of a seabed characterized by high stiffness due to the choice of fixed boundary condition at the base of the structure. For more realistic modelling of seabed material and foundation, enhanced boundary condition can be used.

Competing interests

The authors declare that there is no competing interest regarding the publication of this paper.

References

[1] El Kaddah, N.H. (1983). Water wave-structure interaction for small amplitude structural oscillations. Doctoral thesis, City University London.

[2] Graff, K. F. (1975). Wave motions in elastic solids, Clarendon Press.

[3] Massel S.R, (1989). Hydrodynamics of Coastal Zones, Elsevier.

[4] Dean, R.G., Dalrymple R.A. (1991). Water wave mechanics for engineers and scientists, World Scientific.

[5] Det Norske Veritas Recommended Practice DNV-RP-C205 (2010), Environmental Conditions and Environmental Loads, DNV-RP-C205, October 2010.

[6] Pavlou D. G. (2015). Essentials of the Finite Element Method for Mechanical and Structural Engineers, Elsevier.

[7] Oberhettinger F., Badii L. (1973). Tables of Laplace Transforms. Berlin Heidelberg, New York.

[8] Cheng H-D., Sidauruk P. (1994). Approximate Inversion of the Laplace Transform, THE MATHEMATICA JOURNAL, Miller Freeman Publications.

[9] T. Giotis, D. Pavlou and K. A. Belibassakis (2019). Flexural dynamic behavior of submerged cylindrical structures under wave loads, IOP Conference Series: Materials Science and Engineering.

To cite: T. Giotis and D. Pavlou. Flexural dynamic response of monopile foundations under linear wave loads. *Pipeline Science and Technology*. 2020; 4(1): 44-50.
http://doi.org/10.28999/2514-541X-2020-4-1-44-50